Computational and Theoretical Chemistry 1062 (2015) 65–73

Contents lists available at ScienceDirect

Computational and Theoretical Chemistry

journal homepage: www.elsevier.com/locate/comptc

Quantum chemical characterization of the $CF_2(OH)CF_2OONO_2$ and $CF_3CF_2OONO_2$ peroxynitrates and related radicals

Rosa Isabel Delvalle Mongelós [a], María Paula Badenes [b,*]

[a] Departamento de Química, Facultad de Ciencias Exactas y Naturales, Universidad Nacional de Asunción, 2189 Campus Universitario San Lorenzo, Paraguay
[b] Instituto de Investigaciones Fisicoquímicas Teóricas y Aplicadas (INIFTA), Departamento de Química, Facultad de Ciencias Exactas, Universidad Nacional de La Plata, Casilla de Correo 16, Sucursal 4, 1900 La Plata, Argentina

ARTICLE INFO

Article history:
Received 16 March 2015
Accepted 26 March 2015
Available online 9 April 2015

Keywords:
$CF_2(OH)CF_2OONO_2$
$CF_3CF_2OONO_2$
Fluorinated peroxynitrates
Quantum-chemical calculations
Enthalpy of formation

ABSTRACT

We present a detailed study of the molecular conformations, vibrational spectra and thermochemistry of the $CF_2(OH)CF_2OONO_2$ and $CF_3CF_2OONO_2$ peroxynitrates. In addition, we studied the $CF_2(OH)CF_2OO$, $CF_2(OH)CF_2O$, CF_3CF_2OO and CF_3CF_2O radicals, formed by the rupture of O—N and O—O bonds of the above peroxynitrates. The geometric structures of the most stable conformations were determined by density functional theory calculations. At the B3LYP/6-311++G(3df,3pd) level of theory, both peroxynitrates present dihedral angle COON values of about 104°. At the best levels of theory employed, G3(MP2)B3 and G4(MP2), the standard enthalpies of formation at 298 K derived from isodesmic reactions, are −265.6, −248.6 and −248.5 kcal mol^{-1} for $CF_2(OH)CF_2OONO_2$, $CF_2(OH)CF_2OO$ and $CF_2(OH)CF_2O$ respectively; while for $CF_3CF_2OONO_2$, CF_3CF_2OO and CF_3CF_2O the values of −268.2, −252.6 and −251.9 kcal mol^{-1} were obtained. Bond dissociation enthalpies of 25.1 and 35.0 kcal mol^{-1} have been predicted for the first time for $CF_2(OH)CF_2OO—NO_2$ and $CF_2(OH)CF_2O—ONO_2$ and of 23.7 and 34.2 kcal mol^{-1} have been estimated for $CF_3CF_2OO—NO_2$ and $CF_3CF_2O—ONO_2$. The obtained result of the dissociation enthalpy of $CF_3CF_2OO—NO_2$ is in excellent agreement with the available experimental determination. Therefore, the O—N bond fission is the primary thermal dissociation pathway for both studied peroxynitrates.

1. Introduction

Since long time there are evidences of the atmospheric degradation of chlorofluorocarbons, CFCs [1,2]. Several hydrochlorofluorocarbons, HCFCs, and hydrofluorocarbons, HFCs, where neither chlorine nor bromine are present, have been proposed as substitutes of CFCs. This therefore implies the need of counting on with thermodynamic and kinetic information of degradation processes of those compounds and of the radicals formed from them. In particular, various fluorinated radicals are expected to be intermediates in the atmospheric oxidation of HCFCs and HFCs [3–11]. Subsequently, under atmospheric conditions these radicals add O_2 to form fluoroperoxy radicals [12–14]. Then, they can react with NO, NO_2, HO_2 or other peroxy radicals. The reaction with NO_2 gives the corresponding peroxynitrates, $ROONO_2$, which may act as reservoir of both RO_2 as NO_2 radicals being able to transport NO_2 over large distances from polluted to unpolluted areas [15,16].

To date, several fluoroperoxynitrates are known, as for example CF_3OONO_2 [13,17], $CF_3C(O)OONO_2$ [18], $CF_3CF_2OONO_2$ [19], and $CF_3CF_2C(O)OONO_2$ [20]. In a work about the kinetics of the gas-phase reactions of tetrafluoroethylene with the OH and NO_3 radicals, the observed spectral features allowed to identify a new peroxynitrate, $CF_2(OH)CF_2OONO_2$ [21]. To our knowledge, no experimental or theoretical data about conformations, molecular structure or thermochemistry of $CF_2(OH)CF_2OONO_2$ and related $CF_3CF_2OONO_2$ peroxynitrate have been reported. Therefore, this work is concerned with a quantum chemical study of the characterization of the above peroxynitrates and the radicals generated by the rupture of the O—O and O—N bonds. In particular, the molecular conformations, vibrational spectra and thermochemistry of $CF_2(OH)CF_2OONO_2$, $CF_2(OH)CF_2OO$ and $CF_2(OH)CF_2O$ species have been determined for the first time.

2. Computational details

All quantum-chemical calculations were carried out using the Gaussian 09 computational package [22]. The potential energy curves for the internal rotations of the $CF_2(OH)CF_2OONO_2$, $CF_2(OH)CF_2OO$, $CF_2(OH)CF_2O$, $CF_3CF_2OONO_2$, CF_3CF_2OO and CF_3CF_2O species were computed at the B3LYP level of theory using the 6-311++G(3df,3pd) triple split valence basis set [23]. This

* Corresponding author. Tel.: +54 221 4257430; fax: +54 221 4254642.
E-mail address: mbadenes@inifta.unlp.edu.ar (M.P. Badenes).

http://dx.doi.org/10.1016/j.comptc.2015.03.024
2210-271X/

well-known Becke's three-parameter hybrid functional [24,25] is coupled to the correlation functional of Lee, Yang and Parr [26]. The selected basis set represents appropriately both the region between the bonded atoms, and the region that is far from the nuclei. Molecular geometries were fully optimized using analytical gradient methods, while harmonic vibrational frequencies were derived via analytical second derivatives methods. These frequencies, used to evaluate the zero-point energies (ZPE) and the vibrational contribution to the thermal correction at 298.15 K, were not scaled. The geometric parameters and vibrational frequencies were also computed using the M06-2X functional, which offers double amount of nonlocal exchange (2X) [27]. This functional is recommended most highly for the study of the structures and thermochemistry of the main-group elements [27].

Hybrid approaches were compared with those derived from the more accurate G3(MP2)B3 [28,29] and G4(MP2) [30] *ab initio* methods. The G3(MP2)B3 model employs the B3LYP functional in combination with the 6-31G(d) basis set to compute the optimized geometric parameters and harmonic vibrational frequencies (scaled by a factor 0.96). Then, a set of single-point energy evaluations are included and the final energy is comparable to that computed at the high-level QCISD(T, full)/G3Large. Thus, the average absolute deviation from well-known experimental enthalpies of formation is 1.13 kcal mol^{-1} [28]. This model accounts for spin–orbit, core and higher-level corrections [28,29]. On the other hand, the G4(MP2) procedure is based on G4 theory, in which the MP3 and MP4 large basis set calculations are eliminated [30]. Its aim is to approximate at the CCSD(T) level with a large basis set, through a series of single point energy calculations at lower levels of theory using geometric structures and harmonic vibrational frequencies (scaled by 0.9854) computed at the B3LYP/6-31G(2df,p) level. The G4(MP2) model is very successful in improving the prediction of thermochemical properties, with an average absolute deviation of 1.04 kcal mol^{-1} [30].

3. Results and discussion

3.1. Torsional barriers

$CF_2(OH)CF_2OONO_2$ presents five internal rotations around the C—OH, C—C, C—OO, O—N and O—O bonds and may adopt several conformations. To determine the most stable conformer, the potential energy for all internal rotations were calculated at both B3LYP/6-311++G(d,p) and B3LYP/6-311++G(3df,3pd) levels of theory allowing the molecular geometry to relax on changing the torsion angles between 0° and 360° in steps of 15°. In addition, the molecular structures at the minima (different rotational conformers) and at the maxima (transition states) of potential energy curves were fully optimized at the B3LYP/6-311++G(3df,3pd) level of theory. Thus, it was possible to identify the seven different conformers shown in the Fig. 1. For comparative purposes, a similar study for the related $CF_3CF_2OONO_2$ molecule was done. This peroxynitrate presents four internal rotations around the C—C, C—O, O—N and O—O bonds.

In a similar way, we studied the internal rotations of the $CF_2(OH)CF_2OO$, $CF_2(OH)CF_2O$, CF_3CF_2OO and CF_3CF_2O radicals, generated by the rupture of O—N and O—O bonds in $CF_2(OH)CF_2OONO_2$ and $CF_3CF_2OONO_2$, respectively. The $CF_2(OH)CF_2OO$ radical presents three internal rotations around C—OH, C—C and C—OO bonds, while $CF_2(OH)CF_2O$ exhibits only two rotations about C—OH and C—C bonds. In the case of CF_3CF_2OO and CF_3CF_2O radicals it is observed the same internal rotations except those corresponding to the C—OH bonds.

The calculated rotational potentials curves at the B3LYP/6-311++G(3df,3pd) level of theory, shown in the Figs. 2–6, were fitted to a truncated Fourier expansion,

$$V(\Phi) = a_0 + \Sigma a_i \cos(i\Phi) + \Sigma b_i \sin(i\Phi) \quad (1)$$

where V is the relative energy at torsional angle Φ and i = 1–4. For all cases, the squared correlation coefficients r^2 values better than 0.99 were obtained. The resulting values for the a_i and b_i coefficients at the B3LYP/6-311++G(3df,3pd) level of $CF_2(OH)CF_2OONO_2$ are listed in Table A and the corresponding to $CF_2(OH)CF_2OO$ and $CF_2(OH)CF_2O$ radicals in Table B of the Supplementary material.

Both peroxynitrates present practically identical potential barriers for internal rotations. Thus, we only discuss the potential energy curves computed for the novel $CF_2(OH)CF_2OONO_2$ peroxynitrate and the corresponding radicals, while the potential curves for $CF_3CF_2OONO_2$, CF_3CF_2OO and CF_3CF_2O (Figs. A–D) and values for the a_i and b_i coefficients at the B3LYP/6-311+G(3df) level of theory (Tables C and D) are given in the Supplementary material.

Fig. 2a shows the calculated rotational barriers around the C—OH bond for $CF_2(OH)CF_2OONO_2$. As can see, the symmetrical potential curve presents three minima at CC—OH dihedral angle of 181°, 59° and 302° (conformers 1, 2 and 3 of Fig. 1, respectively) separated by barriers of 1.4 kcal mol^{-1} (at 112° and 251°) and 2.0 kcal mol^{-1} (at 358°) at the B3LYP/6-311++G(3df,3pd) level. The imaginary vibrational frequencies for these transition states are ν = 261i, 244i and 303i cm^{-1}, respectively. The minima possess a difference of energy with regard to conformer 1 of 0.69 and 0.72 kcal mol^{-1}, as it is indicated in the Fig. 1. The corresponding potentials of $CF_2(OH)CF_2OO$ and $CF_2(OH)CF_2O$ radicals are shown in the Fig. 2b. The potential curve of $CF_2(OH)CF_2OO$ presents characteristic very similar to the previous one but the barrier height at about 360° is higher (2.5 kcal mol^{-1} and ν = 329i cm^{-1}), while the aspect of the curve of $CF_2(OH)CF_2O$ is completely different. In the latter case, the interaction between fluorine and hydrogen atom of OH group appears to be the determinant aspect in the form of the potential. This potential curve presents two minima at the same energy and two barriers of 2.7 and 3.2 kcal mol^{-1} (ν = 423i and 135i cm^{-1}) at the B3LYP/6-311++G(3df,3pd) level.

The calculated rotational barriers around the C—C bond are shown in Fig. 3. This rotation leads to three different conformers for $CF_2(OH)CF_2OONO_2$ at FC—CO dihedral angles of 65°, 182° and 303° (Fig. 3a), being the first the most stable conformer (conformer 1). The other conformers are 0.04 and 0.27 kcal mol^{-1} less stable as calculated at the B3LYP/6-311++G(3df,3pd) level (conformers 4 and 5). The barriers in this curve, at dihedral angles of 124°, 243° and 296°, are of 3.6 kcal mol^{-1} with ν = 56i cm^{-1} at the same level. Additionally, in Fig. 3b are shown the calculated rotational potentials around C—C bond for $CF_2(OH)CF_2OO$ and $CF_2(OH)CF_2O$ radicals. The form of these potential curves are very similar to the corresponding to $CF_2(OH)CF_2OONO_2$. In the case of $CF_2(OH)CF_2OO$, the barrier heights are slightly higher, of 3.8 kcal mol^{-1} (ν = 62i cm^{-1}), but for $CF_2(OH)CF_2O$ are about 60% higher (5.7 kcal mol^{-1} and ν = 60i cm^{-1}) at the B3LYP/6-311++G(3df,3pd) level.

Fig. 4 shows the potential curves computed for the rotation about C—O bond in both (a) $CF_2(OH)CF_2OONO_2$ and (b) $CF_2(OH)CF_2OO$. These potentials present three minima and three maxima. The conformers 6 and 7 (at CC—OO dihedral angles of 76° and 283°) of $CF_2(OH)CF_2OONO_2$ are 1.80 and 2.76 kcal mol^{-1} less stable than conformer 1 (at 183°) and the barriers at about 126°, 243° and 355° present values of 3.6 (41i cm^{-1}), 4.5 (52i cm^{-1}), and 4.7 kcal mol^{-1} (48i cm^{-1}), respectively. In the case of $CF_2(OH)CF_2OO$, the minima show smaller energy difference each other, of 0.9 and 0.7 kcal mol^{-1} at 81° and 286° with regard to the most stable at about 181° at the B3LYP/6-311++G(3df,3pd) level. And the transitions states appear at similar dihedral angles (of 124°, 237° and 5°) but the barrier heights also are smaller, of 1.7, 1.8 and 3.4 kcal mol^{-1} respectively (with ν values of 79i, 80i and 94i cm^{-1}).

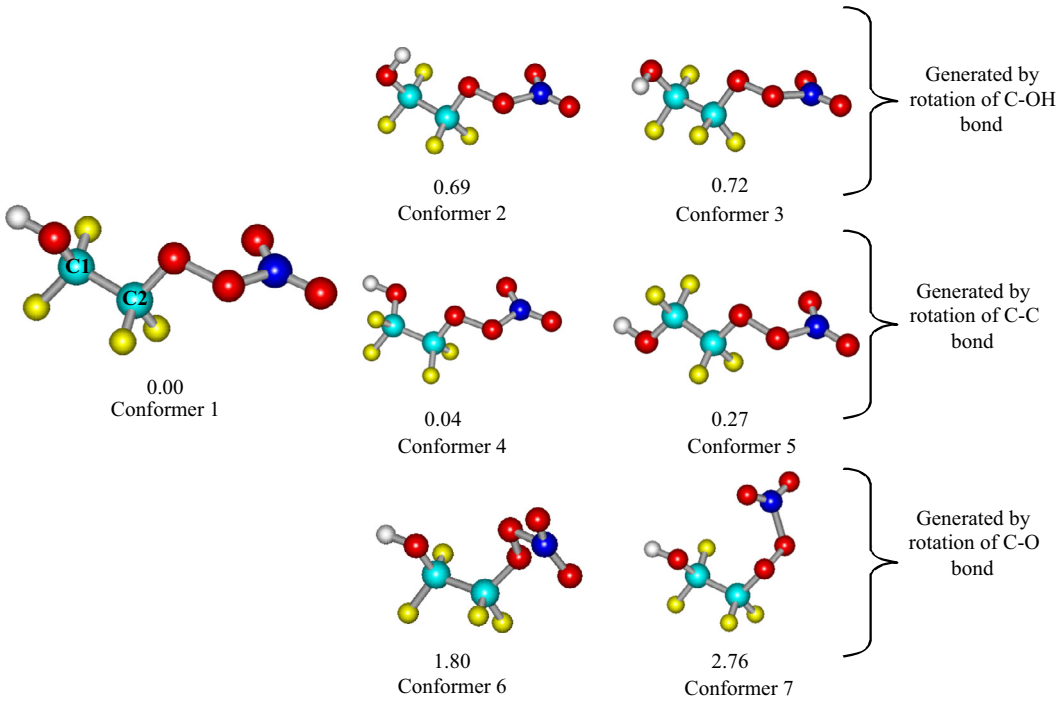

Fig. 1. Molecular geometries and relative energies of the different conformers of $CF_2(OH)CF_2OONO_2$ optimized at the B3LYP/6-311++G(3df,3pd) level of theory.

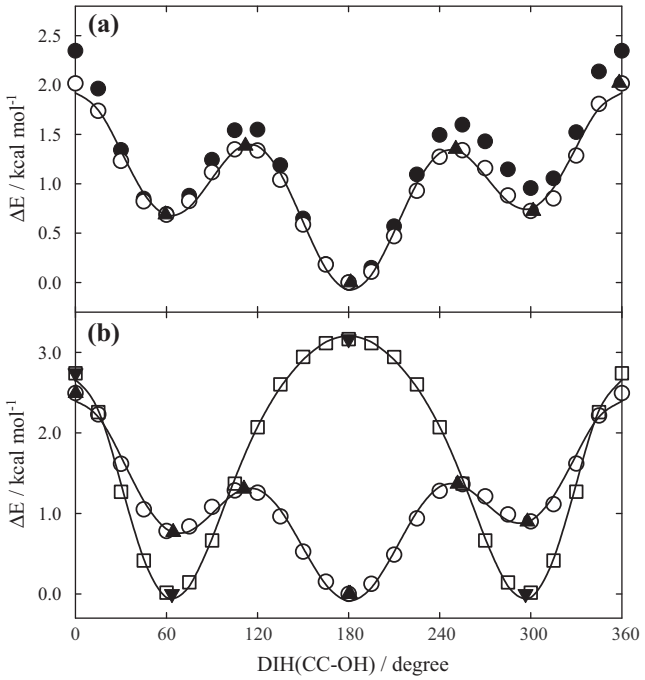

Fig. 2. Potential energy barriers for internal rotation around C—OH bond for (a) $CF_2(OH)CF_2OONO_2$ and (b) $CF_2(OH)CF_2OO$ and $CF_2(OH)CF_2O$ radicals. In (a), black circles: B3LYP/6-311++G(d,p), open circles: B3LYP/6-311++G(3df,3pd). In (b), open circles: $CF_2(OH)CF_2OO$ at the B3LYP/6-311++G(3df,3pd) level, open squares: $CF_2(OH)CF_2O$ at the same level. Triangles: full optimized at the B3LYP/6-311++G(3df,3pd) level. Lines: Fourier analysis with the coefficients of Tables A and B of the Supplementary material.

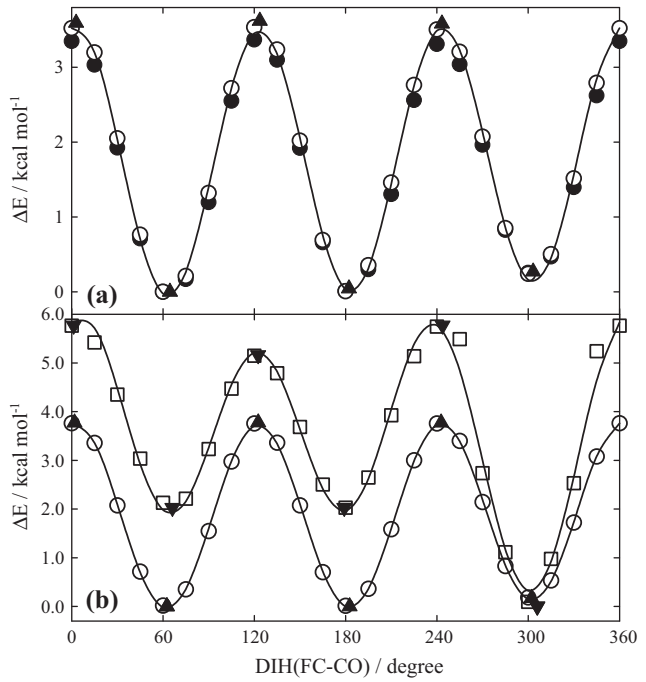

Fig. 3. Potential energy barriers for internal rotation around C—C bond for (a) $CF_2(OH)CF_2OONO_2$ and (b) $CF_2(OH)CF_2OO$ and $CF_2(OH)CF_2O$ radicals. In (a), black circles: B3LYP/6-311++G(d,p), open circles: B3LYP/6-311++G(3df,3pd). In (b), open circles: $CF_2(OH)CF_2OO$ at the B3LYP/6-311++G(3df,3pd) level, open squares: $CF_2(OH)CF_2O$ at the same level. Triangles: full optimized at the B3LYP/6-311++G(3df,3pd) level. Lines: Fourier analysis with the coefficients of Tables A and B of the Supplementary material.

In the case of the rotation around the O—N bond, the symmetric potential energy curve of the Fig. 5 was calculated. Rotational barriers of 9.1 kcal mol^{-1} (ν = 84i cm^{-1}) were computed at the B3LYP/6-311++G(3df,3pd) level and the observed two minima are equivalent (conformer 1). This is because of rotating group, NO_2, possesses an axis of symmetry and its rotation does not lead to different conformers.

Finally, Fig. 6 shows the typical potential energy curve calculated for internal rotation around O—O bond in a peroxynitrate or in a peroxide [31–33]. This rotation leads to two minima (optical

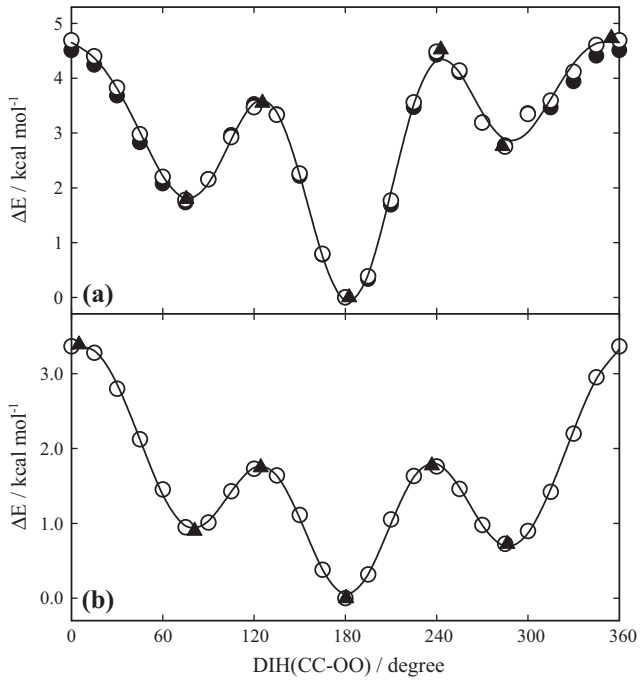

Fig. 4. Potential energy barriers for internal rotation around C—O bond for (a) $CF_2(OH)CF_2OONO_2$ and (b) $CF_2(OH)CF_2OO$ radical. Black circles: B3LYP/6-311++G(d,p), open circles: B3LYP/6-311++G(3df,3pd), triangles: full optimized at the B3LYP/6-311++G(3df,3pd) level. Lines: Fourier analysis with the coefficients of Tables A and B of the Supplementary material.

isomers). They are separated by a high electronic barrier of 16.4 kcal mol^{-1} (ν = 179i cm^{-1}) at a dihedral angle of about 0.7° and a lower barrier of 4.5 kcal mol^{-1} (ν = 54i cm^{-1}) at about 180°.

3.2. Molecular structures and harmonic vibrational frequencies

As Fig. 1 shows, the most stable conformation of $CF_2(OH)CF_2OONO_2$ corresponds to CCOH and CCOO dihedral angles of about 180°. The geometrical parameters together with the corresponding to $CF_2(OH)CF_2OO$ and $CF_2(OH)CF_2O$ radicals, derived at the B3LYP/6-311++G(3df,3pd) and M06-2X/6-311++G(3df,3pd) levels are presented in Table 1. The skeleton is very similar to

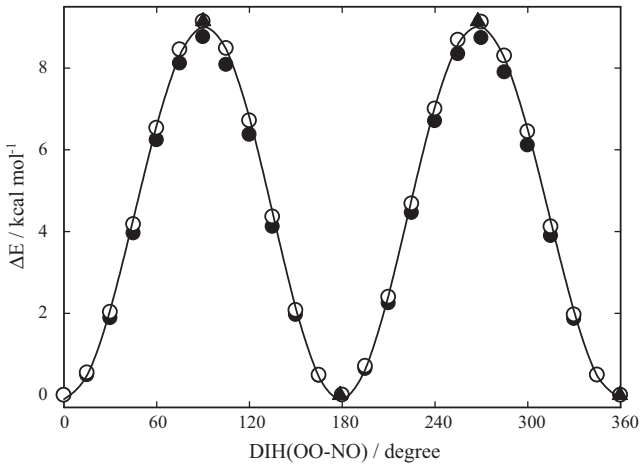

Fig. 5. Potential energy barriers for internal rotation around O—N bond for $CF_2(OH)CF_2OONO_2$. Black circles: B3LYP/6-311++G(d,p), open circles: B3LYP/6-311++G(3df,3pd), triangles: full optimized at the B3LYP/6-311++G(3df,3pd) level. Line: Fourier analysis with the coefficients of Table A of the Supplementary material.

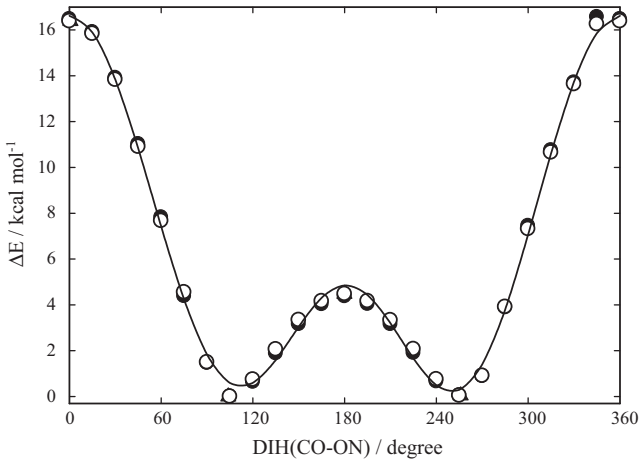

Fig. 6. Potential energy barriers for internal rotation around O—O bond for $CF_2(OH)CF_2OONO_2$. Black circles: B3LYP/6-311++G(d,p), open circles: B3LYP/6-311++G(3df,3pd), triangles: full optimized at the B3LYP/6-311++G(3df,3pd) level. Line: Fourier analysis with the coefficients of Table A of the Supplementary material.

Table 1
Geometrical parameters of $CF_2(OH)CF_2OONO_2$, $CF_2(OH)CF_2OO$ and $CF_2(OH)CF_2O$ calculated at the B3LYP/6-311++G(3df,3pd) and M06-2X/6-311++G(3df,3pd) levels of theory (bond lengths in Angstroms and angles in degrees).

Parameter	$CF_2(OH)CF_2OONO_2$		$CF_2(OH)CF_2OO$		$CF_2(OH)CF_2O$	
	B3LYP	M06-2X	B3LYP	M06-2X	B3LYP	M06-2X
r(C1—C2)	1.560	1.544	1.555	1.542	1.674	1.586
$r(C1—F)_{mean}$	1.355	1.342	1.356	1.343	1.331	1.330
r(C1—O)	1.344	1.341	1.344	1.340	1.341	1.343
r(O—H)	0.966	0.965	0.966	0.965	0.967	0.965
$r(C2—F)_{mean}$	1.340	1.329	1.329	1.321	1.364	1.345
r(C2—O)	1.388	1.383	1.428	1.410	1.270	1.315
r(O—O)	1.406	1.383	1.320	1.303	–	–
r(N—O)	1.538	1.468	–	–	–	–
$r(N=O)_{mean}$	1.182	1.177	–	–	–	–
$\angle(FC1C2)_{mean}$	108.4	108.2	108.4	108.3	108.1	108.4
$\angle(C1C2F)_{mean}$	109.8	109.9	110.4	110.3	105.2	107.5
∠(OC1C2)	109.6	109.4	109.5	109.2	108.8	110.3
∠(C1C2O)	106.9	106.9	107.1	107.3	106.3	107.9
∠(C1OH)	109.6	109.6	109.8	110.0	110.0	110.1
∠(C2OO)	109.0	108.3	110.7	110.2	–	–
∠(OON)	109.0	108.9	–	–	–	–
$\angle(ON=O)_{mean}$	112.5	113.1	–	–	–	–
DIH(FC1C2O)	64.6	64.6	62.6	63.1	-54.1	−52.4
DIH(HOC1C2)	−178.6	−178.6	−179.0	−179.3	63.6	60.4
DIH(C1C2OO)	−177.5	−173.6	−179.5	−179.4	–	–
DIH(C2OON)	103.9	100.8	–	–	–	–
DIH(OON=O)	178.5	178.6	–	–	–	–

the predicted for the $CF_3CF_2OONO_2$ whose structural parameters, together with those corresponding to related radicals, are listed in Table 2. Both peroxynitrates present COON dihedral angles of 104° at the B3LYP/6-311++G(3df,3pd) level, as it is usual for this type of species. For comparison, CF_3OONO_2 possesses a COON dihedral angle of 105.1° [17].

The novel peroxynitrate $CF_2(OH)CF_2OONO_2$ exhibits a rather long O—N bond of 1.538 Å and a short O—O bond of 1.406 Å at the B3LYP/6-311++G(3df,3pd) level. Both values are very close to the related peroxynitrates $CF_3CF_2OONO_2$ (Table 2) and CF_3OONO_2 (1.523 and 1.414 Å) [17]. The difference between those bonds suggests a primary thermal dissociation pathway for $CF_2(OH)CF_2OONO_2$ into $CF_2(OH)CF_2OO$ and NO_2.

Calculated harmonic vibrational frequencies, infrared intensities and approximate mode assignments for the most stable

Table 2
Geometrical parameters of $CF_3CF_2OONO_2$, CF_3CF_2OO and CF_3CF_2O calculated at the B3LYP/6-311+G(3df) and M06-2X/6-311+G(3df) levels of theory (bond lengths in Angstroms and angles in degrees).

Parameter	$CF_3CF_2OONO_2$		CF_3CF_2OO		CF_3CF_2O	
	B3LYP	M06-2X	B3LYP	M06-2X	B3LYP	M06-2X
r(C1—C2)	1.561	1.546	1.556	1.543	1.606	1.569
$r(C1—F)_{mean}$	1.330	1.320	1.330	1.321	1.330	1.318
$r(C2—F)_{mean}$	1.339	1.328	1.328	1.320	1.358	1.337
r(C2—O)	1.385	1.380	1.425	1.408	1.315	1.332
r(O—O)	1.406	1.383	1.321	1.304	–	–
r(N—O)	1.547	1.473	–	–	–	–
$r(N=O)_{mean}$	1.180	1.176	–	–	–	–
$\angle(FC1C2)_{mean}$	109.8	109.6	109.8	109.6	109.5	109.5
$\angle(C1C2F)_{mean}$	109.5	109.7	110.2	110.0	107.6	108.2
∠(C1C2O)	106.6	106.5	106.8	106.8	106.8	106.9
∠(C2OO)	109.1	108.4	110.7	110.2	–	–
∠(OON)	108.9	108.8	–	–	–	–
$\angle(ON=O)_{mean}$	112.3	113.0	–	–	–	–
DIH(FC1C2O)	61.4	62.1	60.3	60.2	60.6	60.3
DIH(C1C2OO)	−178.1	−174.4	−179.6	−180.0	–	–
DIH(C2OON)	104.0	101.0	–	–	–	–
DIH(OON=O)	178.3	178.3	–	–	–	–

conformers of $CF_2(OH)CF_2OONO_2$, $CF_3CF_2OONO_2$ and related oxy and peroxy radicals are listed in Tables 3 and 4. A comparison between computed and experimental frequencies for $CF_3CF_2OONO_2$ leads to mean deviations of 46 and 111 cm^{-1} at the B3LYP/6-311+G(3df) and M06-2X/6-311+G(3df), respectively. At these levels of theory, the frequency scaling factors are expected to be close to unity [34]. Mode assignments were obtained from the animation of the normal modes and by comparison with species with similar groups. However, most of the modes are strongly mixed and therefore given assignments are only approximate. The asymmetrical NO_2 stretching mode of both peroxynitrates are located at wavenumbers slightly higher than other alkyl-peroxynitrates but the calculated values are similar to observed for fluorinated acyl-peroxynitrates, like $CF_3CF_2C(O)OONO_2$ (at 1849 cm^{-1}) [17,20]. In particular, the calculated value of 1830 cm^{-1} for $CF_2(OH)CF_2OONO_2$ result about 6% higher than the observed value of 1718 cm^{-1} [21]. However, the symmetrical NO_2 stretching modes agree very well with wavenumbers observed for other fluorinated alkyl-peroxynitrates like $CF_3CF_2CF_2OONO_2$ (1302 cm^{-1}) [35], $CF_3CF_2OONO_2$ (1304 cm^{-1}) [19] and CF_3OONO_2 (1314 cm^{-1}) [17]. Also the C—O and O—O stretching modes appear at about 850 and 950 cm^{-1}, like other fluorinated peroxynitrates [17,35]. Finally, the calculated frequencies for the $CF_2(OH)CF_2OO$, $CF_2(OH)CF_2O$, CF_3CF_2OO and CF_3CF_2O radicals are observed at wavenumbers similar to the corresponding modes in $CF_2(OH)CF_2OONO_2$ and $CF_3CF_2OONO_2$.

3.3. Thermochemistry

To estimate the enthalpy changes for the possible decomposition channels of $CF_2(OH)CF_2OONO_2$ and $CF_3CF_2OONO_2$, the standard enthalpies of formation at 298 K, $\Delta H_{f,298}$, for both peroxynitrates and related oxy and peroxy radicals were first

Table 3
Harmonic vibrational frequencies (in cm^{-1}), approximated assignments and infrared intensities (between parenthesis, in km mol^{-1}) for $CF_2(OH)CF_2OONO_2$, $CF_2(OH)CF_2OO$ and $CF_2(OH)CF_2O$ at the B3LYP/6-311++G(3df,3pd) and M06-2X/6-311++G(3df,3pd) levels.

Approximated assignments	$CF_2(OH)CF_2OONO_2$		$CF_2(OH)CF_2OO$		$CF_2(OH)CF_2O$	
	B3LYP	M06-2X	B3LYP	M06-2X	B3LYP	M06-2X
Str. O—H	3784 (106)	3853 (132)	3784 (104)	3835 (124)	3778 (148)	3846 (134)
Str. asym. NO_2	1830 (412)	1888 (498)	–	–	–	–
Str. C—C	1447 (31)	1503 (24)	1456 (29)	1513 (22)	1334 (168)	1340 (309)
Str. sym. NO_2	1358 (255)	1420 (254)	–	–	–	–
Str. C—OH	1247 (272)	1313 (317)	1246 (353)	1308 (75)	1243 (288)	1285 (159)
Str. sym. $C1F_2$	1235 (119)	1291 (56)	994 (249)	1053 (195)	1388 (167)	1418 (175)
Str. asym. $C1F_2$	1175 (263)	1261 (293)	1208 (264)	1287 (247)	1109 (259)	1199 (255)
Str. asym. $C2F_2$	1130 (60)	1212 (125)	1258 (58)	1315 (334)	1074 (176)	1156 (181)
Str. asym. $C1F_2$	1109 (415)	1196 (354)	1109 (205)	1206 (165)	–	–
Str. sym. $C1F_2$	1019 (243)	1092 (72)	1063 (141)	1150 (242)	1006 (341)	1097 (280)
Str. O—O	965 (10)	1050 (117)	1165 (45)	1240 (96)	–	–
Str. C2—O	839 (7)	878 (40)	821 (2)	863 (2)	877 (50)	971 (42)
Bend. NO_2	806 (188)	862 (208)	–	–	–	–
Out of plane N	733 (11)	792 (11)	–	–	–	–
Bend FCOH	718 (58)	752 (7)	718 (50)	740 (56)	735 (78)	819 (15)
Bend NOO	679 (20)	737 (74)	–	–	–	–
Bend FCO	605 (0.3)	631 (4)	601 (0.1)	621 (0.2)	588 (9)	610 (5)
Bend CF_2	590 (11)	623 (9)	591 (4)	615 (4)	591 (3)	696 (15)
Bend. FCOH	548 (19)	585 (11)	544 (16)	558 (20)	523 (11)	531 (3)
Out of plane O1	524 (16)	555 (17)	499 (10)	520 (12)	–	–
Str. O—N	493 (14)	542 (8)	–	–	–	–
Bend. FCC	392 (4)	418 (7)	388 (4)	406 (5)	488 (40)	520 (13)
Bend. CF_2	367 (6)	384 (10)	374 (4)	387 (4)	538 (55)	602 (4)
Rock. NO_2	316 (4)	342 (3)	–	–	–	–
Out of plane O2	302 (2)	320 (14)	–	–	–	–
Bend. COO	–	–	348 (2)	360 (3)	–	–
Bend. COH	253 (50)	300 (73)	–	–	–	–
Bend FCC	–	–	300 (2)	312 (2)	230 (2)	234 (7)
Torsion C—OH	245 (55)	281 (14)	240 (101)	246 (113)	327 (62)	346 (1)
Wag. CF_2	225 (2)	229 (0.9)	225 (8)	230 (0.2)	391 (85)	387 (32)
Bend. CCO	178 (0.7)	187 (0.7)	173 (0.3)	179 (0.3)	352 (2)	365 (22)
Deformation	–	–	–	–	290 (12)	318 (78)
Wag. CF_2	–	–	–	–	206 (8)	218 (9)
Torsion O—O	97 (0.03)	100 (0.02)	–	–	–	–
Torsion O—N	75 (0.1)	80 (0.1)	–	–	–	–
Torsion C—C	54 (0.1)	58 (0.1)	63 (0.01)	73 (0.004)	71 (0.8)	71 (0.8)
Torsion C—O	47 (0.5)	50 (0.2)	104 (0.03)	132 (0.04)	–	–

Table 4
Harmonic vibrational frequencies (in cm^{-1}), approximated assignments and infrared intensities (between parenthesis, in km mol^{-1}) for $CF_3CF_2OONO_2$, CF_3CF_2OO and CF_3CF_2O at the B3LYP/6-311+G(3df) and M06-2X/6-311+G(3df) levels.

Approximated assignments	$CF_3CF_2OONO_2$			CF_3CF_2OO		CF_3CF_2O	
	B3LYP	M06-2X	Exp. [19]	B3LYP	M06-2X	B3LYP	M06-2X
Str. asym. NO_2	1839 (412)	1895 (499)	1764	–	–	–	–
Str. C—C	1368 (102)	1451 (22)		1375 (31)	1460 (24)	1277 (132)	1349 (199)
Str. sym. NO_2	1347 (194)	1418 (262)	1304	–	–	–	–
Str. asym. CF_3	1219 (321)	1303 (333)	1244	1223 (504)	1305 (493)	1235 (344)	1306 (333)
Str. asym. CF_3	1215 (192)	1298 (218)	1188	1221 (165)	1304 (195)	1223 (254)	1303 (193)
Str. asym. CF_2	1176 (150)	1267 (125)	1085	1206 (9)	1288 (18)	1120 (177)	1232 (159)
Str. sym. CF_2	1164 (266)	1242 (265)		1022 (284)	1098 (302)	670 (8)	712 (43)
Str. sym. CF_3	1079 (376)	1144 (315)		1184 (248)	1259 (211)	1083 (380)	1188 (307)
Str. O—O	969 (20)	1075 (20)		1119 (47)	1199 (82)	–	–
Str. C—O	841 (5)	879 (29)		822 (0.6)	864 (0.2)	917 (25)	1049 (28)
Bend. NO_2	804 (192)	860 (217)	790	–	–	–	–
Umbrella CF_3	746 (35)	791 (14)		745 (27)	769 (34)	774 (27)	833 (1)
Out of plane N	730 (9)	772 (29)		–	–	–	–
Bend NOO	678 (13)	743 (20)		–	–	–	–
Bend FCO	605 (0.3)	630 (4)		–	–	582 (4)	608 (1)
Bend CF_2	588 (7)	622 (7)		599 (0.01)	620 (0.04)	599 (0.6)	619 (0.4)
Bend CF_2	538 (10)	583 (12)		591 (3)	614 (2)	516 (3)	532 (7)
Out of plane O1	520 (11)	547 (7)		495 (4)	514 (6)	–	–
Bend FCO	–	–		–	–	509 (1)	516 (3)
Str. O—N	486 (19)	535 (2)		–	–	–	–
Wag. CF_2	387 (0.2)	411 (0.01)		370 (0.002)	384 (0.001)	352 (0.002)	369 (0.0)
Bend. CF_2	359 (0.8)	376 (0.7)		534 (6)	548 (8)	–	–
Bend. COO	–	–		384 (0.4)	399 (0.8)	–	–
Rock. NO_2	317 (2)	341 (2)		–	–	–	–
Out of plane O2	300 (5)	316 (3)		–	–	–	–
Deformation	248 (2)	283 (0.7)		344 (0.5)	356 (0.6)	328 (0.4)	363 (0.005)
Wag. CF_2	218 (2)	222 (2)		217 (2)	222 (0.001)	210 (2)	344 (0.1)
Bend. FCC	–	–		300 (1)	310 (2)	342 (1)	228 (2)
Deformation	175 (1)	183 (1)		–	–	–	–
Bend. CCO	–	–		170 (2)	173 (2)	228 (1)	217 (2)
Torsion O—O	95 (0.04)	100 (0.01)		–	–	–	–
Torsion O—N	74 (0.1)	82 (0.2)		–	–	–	–
Torsion C—C	53 (0.01)	57 (0.02)		62 (0.01)	61 (0.03)	62 (0.004)	62 (0.003)
Torsion C—O	45 (0.001)	50 (0.07)		103 (0.2)	133 (0.3)	–	

Table 5
Isodesmic reactions, calculated enthalpy changes and enthalpies of formation at 298 K (in kcal mol^{-1}) for $CF_2(OH)CF_2OONO_2$, $CF_2(OH)CF_2OO$ and $CF_2(OH)CF_2O$. B: 6-311++G(3df,3pd).

$CF_2(OH)CF_2OONO_2$
(1) $C_2H_6 + 2\ CF_3OH + HOONO_2 \rightarrow CF_2(OH)CF_2OONO_2 + CF_2H_2 + CH_4 + H_2O$
(2) $C_2H_6 + 2\ CF_3OH + HONO_2 + H_2O_2 \rightarrow CF_2(OH)CF_2OONO_2 + CF_2H_2 + CH_4 + 2\ H_2O$
(3) $C_2F_6 + 2\ CH_3OH + HOONO_2 \rightarrow CF_2(OH)CF_2OONO_2 + 2\ CH_3F + H_2O$

$CF_2(OH)CF_2OO$
(4) $C_2H_6 + 2\ CF_3OH + H_2O_2 + OH \rightarrow CF_2(OH)CF_2OO + CF_2H_2 + CH_4 + 2\ H_2O$
(5) $C_2H_6 + 2\ CF_3OH + H_2O_2 + CH_3O \rightarrow CF_2(OH)CF_2OO + CF_2H_2 + CH_4 + H_2O + CH_3OH$
(6) $C_2H_6 + 2\ CF_3OH + HOO \rightarrow CF_2(OH)CF_2OO + CF_2H_2 + CH_4 + H_2O$

$CF_2(OH)CF_2O$
(7) $C_2H_6 + 2\ CF_3OH + OH \rightarrow CF_2(OH)CF_2O + CF_2H_2 + CH_4 + H_2O$
(8) $C_2H_6 + 2\ CF_3OH + CH_3O \rightarrow CF_2(OH)CF_2O + CF_2H_2 + CH_4 + CH_3OH$
(9) $C_2F_6 + 2\ CH_3OH + OH \rightarrow CF_2(OH)CF_2O + 2\ CH_3F + H_2O$

Reaction	B3LYP/B		M06-2X/B		G3(MP2)B3		G4(MP2)	
	$\Delta H_{r,298}$	$\Delta H_{f,298}$	$\Delta H_{r,298}$	$\Delta H_{f,298}$	$\Delta H_{r,298}$	$\Delta H_{f,298}$	$\Delta H_{r,298}$	$\Delta H_{f,298}$
1	20.1	−263.5	20.9	−262.7	16.8	−266.8	18.9	−264.7
2	13.8	−263.6	16.1	−261.3	10.3	−267.1	12.7	−264.7
3	−3.8	−262.1	−4.4	−262.7	−6.8	−265.1	−6.6	−264.9
Average		−263.1		−262.2		−266.3		−264.8
4	−11.7	−247.1	−7.0	−243.4	−11.1	−246.5	−13.9	−249.3
5	4.7	−245.4	7.1	−243.0	1.9	−248.1	0.2	−249.8
6	21.7	−246.0	24.8	−242.9	19.9	−247.8	17.7	−250.0
Average		−246.2		−243.1		−247.5		−249.7
7	11.3	−250.4	17.5	−244.2	14.2	−247.5	11.9	−249.8
8	27.6	−247.8	31.5	−243.9	27.3	−248.1	26.0	−249.4
9	−12.5	−249.0	−7.8	−244.3	−9.4	−245.9	−13.6	−250.1
Average		−249.1		−244.1		−247.2		−249.8

Table 6
Isodesmic reactions, calculated enthalpy changes and enthalpies of formation at 298 K (in kcal mol^{-1}) for $CF_3CF_2OONO_2$, CF_3CF_2OO and CF_3CF_2O. B: 6-311+G(3df).

$CF_3CF_2OONO_2$
(1) $CH_3CF_3 + CF_3OH + HOONO_2 \rightarrow CF_3CF_2OONO_2 + CH_3F + H_2O$
(2) $C_2F_6 + CH_3OH + HONO_2 + H_2O_2 \rightarrow CF_3CF_2OONO_2 + CH_3F + 2\ H_2O$
(3) $2\ CHF_3 + CH_3CH_2OH + HOONO_2 \rightarrow CF_3CF_2OONO_2 + CH_3F + CH_4 + H_2O$

CF_3CF_2OO
(4) $C_2H_6 + CF_3OH + HOO + CF_2H_2 \rightarrow CF_3CF_2OO + 2\ CH_4 + H_2O$
(5) $C_2F_6 + H_2O_2 + CH_3O \rightarrow CF_3CF_2OO + CH_3F + H_2O$
(6) $C_2F_6 + CH_3OH + HOO \rightarrow CF_3CF_2OO + CH_3F + H_2O$

CF_3CF_2O
(7) $CH_3CF_3 + CH_3O + CF_2H_2 \rightarrow CF_3CF_2O + 2\ CH_4$
(8) $C_2F_6 + CH_3O \rightarrow CF_3CF_2O + CH_3F$
(9) $C_2F_6 + CH_3OH + OH \rightarrow CF_3CF_2O + CH_3F + H_2O$

Reaction	B3LYP/B		M06-2X/B		G3(MP2)B3		G4(MP2)	
	$\Delta H_{r,298}$	$\Delta H_{f,298}$	$\Delta H_{r,298}$	$\Delta H_{f,298}$	$\Delta H_{r,298}$	$\Delta H_{f,298}$	$\Delta H_{r,298}$	$\Delta H_{f,298}$
1	28.2	−265.2	28.5	−264.9	25.1	−268.3	26.5	−266.9
2	−5.4	−266.6	−4.5	−265.7	−8.6	−269.8	−7.8	−269.0
3	3.8	−263.7	1.4	−266.1	−1.0	−268.5	0.8	−266.7
Average		−265.2		−265.6		−268.9		−267.5
4	1.1	−248.0	−1.0	−250.0	−2.7	−251.8	−5.2	−254.3
5	−14.5	−248.4	−15.7	−249.5	−16.8	−250.7	−20.2	−254.1
6	2.4	−249.1	2.1	−249.4	1.1	−250.4	−2.7	−254.2
Average		−248.5		−249.6		−251.0		−254.2
7	−1.1	−246.9	−3.5	−249.2	−4.5	−250.3	−7.0	−252.8
8	8.8	−250.4	9.4	−249.8	8.6	−250.7	5.6	−253.6
9	−7.7	−253.2	−4.6	−250.2	−4.6	−250.1	−8.6	−254.1
Average		−250.2		−249.7		−250.4		−253.5

Table 7
Enthalpies of formation at 298 K [42].

Species	$\Delta H_{f,298}$	Species	$\Delta H_{f,298}$
OH	8.93 ± 0.03	CH_3OH	−48.04 ± 0.14
HOO	2.94 ± 0.06	C_2H_6	−20.04 ± 0.07
H_2O	−57.798 ± 0.009	CH_3F	−57.1 ± 0.2
H_2O_2	−32.48 ± 0.05	CF_3OH	−217.2 ± 0.9
NO_2	8.12 ± 0.02	CHF_3	−165.6 ± 0.5
NO_3	17.9 ± 0.3	CH_3CH_2OH	−56.1 ± 0.1
$HOONO_2$	−12.9 ± 0.6	CF_2H_2	−108.2 ± 0.2
$HONO_2$	−32.1 ± 0.1	CH_3CF_3	−178.2 ± 0.4
CH_4	−17.82 ± 0.01	C_2F_6	−321.3 ± 0.8
CH_3O	5.0 ± 0.5		

determined. To this end, we employed the working isodesmic and isogyric reactions listed in the Tables 5 and 6. In these hypothetical reactions, the number of chemical bonds and the spin multiplicities are conserved. Therefore, some systematic errors due to incompleteness of the basis set and deficiencies in the treatment of the electron correlation energy are cancelled to a great extent [36,37]. The calculated isodesmic enthalpy changes, $\Delta H_{r,298}$, and estimated enthalpies of formation at the employed levels of theory are also included in Tables 5 and 6. In these calculations we have used the reliable experimental enthalpies of formation listed in Table 7 [42]. It should be noted that despite the isodesmic enthalpy change values for the different reactions being quite different (positive or negative), the derived $\Delta H_{f,298}$ values are very close. At the best levels of theory employed here, G3(MP2)B3 and G4(MP2), slightly more negative values than those derived from functionals are obtained. At mentioned levels, the average values of −265.6, −248.6 and −248.5 kcal mol^{-1} for enthalpies of formation of $CF_2(OH)CF_2OONO_2$, $CF_2(OH)CF_2OO$ and $CF_2(OH)CF_2O$ were derived; and the average values of −268.2, −252.6 and −251.9 kcal mol^{-1} for enthalpies of formation of $CF_3CF_2OONO_2$, CF_3CF_2OO and CF_3CF_2O were estimated. The uncertainties in the employed quantum-chemical methods (close to 1 kcal mol^{-1}) and the corresponding to well established enthalpies of formation of the Table 7 (maximum error close to 1 kcal mol^{-1}) suggest conservative error estimates of ±2 kcal mol^{-1}.

For comparison, the standard enthalpies of formation at 298 K were also derived from estimated atomization energies. In this approach the enthalpies of formation at 0 K, $\Delta H_{f,0K}$, were first calculated by subtracting the computed total atomization energies, ΣD_0, from the experimental enthalpies of formation of fluorine (18.47 ± 0.07 kcal mol^{-1}), carbon (169.98 ± 0.1 kcal mol^{-1}), nitrogen (112.53 ± 0.02 kcal mol^{-1}), oxygen (58.99 ± 0.02 kcal mol^{-1}) and hydrogen atoms (51.63 ± 0.001 kcal mol^{-1}) [38]. Then, estimated thermal contributions and $H_{298} - H_{0K}$ values for fluorine, carbon, nitrogen, oxygen and hydrogen atoms of 1.05, 0.25, 1.04, 1.04 and 1.01 kcal mol^{-1} were employed to transform the $\Delta H_{f,0K}$ values to 298 K [39]. The computed ΣD_0, $\Delta H_{f,0K}$ and $\Delta H_{f,298}$ values for $CF_2(OH)CF_2OONO_2$, $CF_3CF_2OONO_2$ and oxy and peroxy radicals are presented in Table 8. This method requires an accurate determination of the energetics of both molecule and constituent atoms [32,33]; therefore it is limited to high level quantum chemical methods and only results derived from the G3(MP2)B3 and G4(MP2) levels of theory are presented here. In fact, with previous methods, good agreement between the enthalpies derived from both total atomization energies and isodesmic reactions approaches is apparent.

The main thermal decomposition channels for both studied peroxynitrates are the breaking of the O—N and O—O bonds. Therefore, to analyze the thermal stability of $CF_2(OH)CF_2OONO_2$ and $CF_3CF_2OONO_2$, we calculated the dissociation enthalpies of the above mentioned bonds. To this, we use the average $\Delta H_{f,298}$ values derived from isodesmic reactions at the G3(MP2)B3 and G4(MP2) levels of theory and the experimental values for NO_2 and NO_3 of the Table 7. In this way, the values of 25.1 and 35.0 kcal mol^{-1} were obtained for the dissociation enthalpies of $CF_2(OH)CF_2OO—NO_2$ and $CF_2(OH)CF_2O—ONO_2$, respectively. And, for the $CF_3CF_2OO—NO_2$ and $CF_3CF_2O—ONO_2$ breakings, the values of 23.7 and 34.2 kcal mol^{-1} were estimated. These results indicate that, as for other peroxynitrates, the O—N bond fission is the more

Table 8
Calculated atomization energies, ΣD_0, and enthalpies of formation at 0 and 298 K for $CF_2(OH)CF_2OONO_2$, $CF_2(OH)CF_2OO$, $CF_2(OH)CF_2O$, $CF_3CF_2OONO_2$, CF_3CF_2OO and CF_3CF_2O (in kcal mol^{-1}).

Level	$CF_2(OH)CF_2OONO_2$			$CF_2(OH)CF_2OO$			$CF_2(OH)CF_2O$		
	ΣD_0	$\Delta H_{f,0K}$	$\Delta H_{f,298}$	ΣD_0	$\Delta H_{f,0K}$	$\Delta H_{f,298}$	ΣD_0	$\Delta H_{f,0K}$	$\Delta H_{f,298}$
G3(MP2)B3	1135.0	−262.0	−266.2	888.0	−245.5	−248.3	830.1	−246.6	−249.0
G4(MP2)	1131.9	−259.0	−263.2	889.6	−247.2	−250.0	831.3	−247.8	−250.3
	$CF_3CF_2OONO_2$			CF_3CF_2OO			CF_3CF_2O		
	ΣD_0	$\Delta H_{f,0K}$	$\Delta H_{f,298}$	ΣD_0	$\Delta H_{f,0K}$	$\Delta H_{f,298}$	ΣD_0	$\Delta H_{f,0K}$	$\Delta H_{f,298}$
G3(MP2)B3	1047.4	−266.6	−270.0	800.3	−250.0	−252.0	742.4	−251.1	−252.8
G4(MP2)	1044.3	−263.5	−267.1	801.9	−251.6	−253.7	743.6	−252.3	−254.1

propitious dissociation channel [31,32,40]. Bossolasco and coworkers studied the synthesis and characterization of $CF_3CF_2OONO_2$ [19]. They determined the rate constant for the thermal decomposition of that peroxynitrate at room temperature as a function of the total pressure and show that reaction is in high-pressure limit above about 80 mbar. The determined activation energy at 250 mbar of 23.11 kcal mol^{-1} is in excellent agreement with the value of 23.7 ± 2 kcal mol^{-1} calculated here. To our knowledge, no experimental or theoretical data about $CF_2(OH)CF_2OONO_2$ have been reported so far. Therefore, the estimations of present work for this new peroxynitrate were derived for the first time. In addition, both determined O—N bond dissociation enthalpies are very close to the value of 25 ± 1 kcal mol^{-1}, proposed for peroxynitrates CX_3OONO_2, with X = F, Cl [41].

The previous dissociation enthalpies of the most probable thermal decomposition channels of $CF_2(OH)CF_2OONO_2$ and $CF_3CF_2OONO_2$, allow for an estimation of their thermal stability at room temperature. Assuming for both peroxynitrates a high pressure pre-exponential value of 2.37×10^{15} s^{-1} [19], as was experimentally determined for $CF_3CF_2OONO_2$, lifetimes of about 18 and 2 min are obtained respectively for $CF_2(OH)CF_2OONO_2$ and $CF_3CF_2OONO_2$ at 298 K. These values suggest that the new peroxynitrate is, at least up about room temperature, a relatively stable species.

4. Conclusions

The present quantum chemical study allowed the structural and thermochemistry characterization of the new peroxynitrate $CF_2(OH)CF_2OONO_2$ and of the related $CF_3CF_2OONO_2$, as well as of the $CF_2(OH)CF_2OO$, $CF_2(OH)CF_2O$, CF_3CF_2OO, and CF_3CF_2O radicals. The calculated geometric structures and harmonic vibrational frequencies of the most stable conformations of the both peroxynitrates present characteristic very similar to other fluorinated peroxynitrates. On the other hand, G3(MP2)B3 and G4(MP2) model chemistry calculations were employed to estimate enthalpies of formation of the studied peroxynitrates and radicals at 298 K. From the isodesmic reaction approach, average values of −265.6, −248.6, −248.5, −268.2, −252.6 and −251.9 kcal mol^{-1} were obtained for $CF_2(OH)CF_2OONO_2$, $CF_2(OH)CF_2OO$, $CF_2(OH)CF_2O$, $CF_3CF_2OONO_2$, CF_3CF_2OO and CF_3CF_2O, respectively, at the mentioned levels of theory. In addition, employing previous enthalpies of formation, dissociation enthalpies of 25.1 and 35.0 kcal mol^{-1} were respectively calculated for $CF_2(OH)CF_2OO—NO_2$ and $CF_2(OH)CF_2O—ONO_2$, while for $CF_3CF_2OO—NO_2$ and $CF_3CF_2O—ONO_2$ values of 23.7 and 34.2 kcal mol^{-1} were estimated. The results present here for the new peroxynitrate $CF_2(OH)CF_2OONO_2$ may aid in its experimental determination.

Acknowledgments

This research project was supported by the Universidad Nacional de La Plata, the Consejo Nacional de Investigaciones Científicas y Técnicas (CONICET) and the Agencia Nacional de Promoción Científica y Tecnológica.

Appendix A. Supplementary material

Coefficients of the Fourier expansion for torsional potentials of $CF_2(OH)CF_2OONO_2$, $CF_2(OH)CF_2OO$ and $CF_2(OH)CF_2O$ at the B3LYP/6-311++G(3df,3pd) level of theory; Potential energy barriers for internal rotations of $CF_3CF_2OONO_2$, CF_3CF_2OO and CF_3CF_2O; and Coefficients of the Fourier expansion for torsional potentials of $CF_3CF_2OONO_2$, CF_3CF_2OO and CF_3CF_2O at the B3LYP/6-311+G(3df) level. Supplementary data associated with this article can be found, in the online version, at http://dx.doi.org/10.1016/j.comptc.2015.03.024.

References

[1] WMO (World Meteorological Organization), Scientific Assessment of Ozone Depletion: 1991, Global Ozone Research and Monitoring Project, Report No. 25, Geneva, Switzerland, 1992.
[2] F.S. Rowland, M.J. Molina, Chlorofluoromethanes in the environment, Rev. Geophys. Space Phys. 13 (1975) 1–35.
[3] J.M. Heras, A.J. Arvia, P.J. Aymonino, H.J. Schumacher, Die Kinetik der Thermischen Reaktion Zwischen Fluor, Kohlenmonoxyd und Sauerstoff, Z. Physik. Chem. NF 28 (1961) 250–261.
[4] A.J. Arvia, P.J. Aymonino, H.J. Schumacher, Die Kinetik der Thermischen Reaktion Zwischen Kohlenmonoxid und Fluormonoxid, Z. Physik. Chem. NF 51 (1966) 170–182.
[5] A.E. Croce, C.A. Tori, E. Castellano, Kinetics of CF_2O production in the gas phase thermal reaction between F_2O and CO inhibited by O_2, Z. Physik. Chem. NF 162 (1989) 161–170.
[6] A.E. Croce, E. Castellano, Kinetics of the gas phase formation of CO_2 in the thermal reaction between CO and O_2 sensitized by $CF_2(OF)_2$, Z. Physik. Chem. 185 (1994) 165–176.
[7] M.M. Maricq, J.J. Szente, G.A. Khitrov, J.S. Francisco, FCO: UV spectrum, self-reaction kinetics and chain reaction with F_2, Chem. Phys. Lett. 199 (1992) 71–77.
[8] M.M. Maricq, J.J. Szente, G.A. Khitrov, J.S. Francisco, Temperature dependent kinetics of the formation and self-reactions of FC(O)O2 and FC(O)O radicals, J. Chem. Phys. 98 (1993) 9522–9531.
[9] T.J. Wallington, T. Ellermann, O.J. Nielsen, J. Sehested, Atmospheric chemistry of FCO_x radicals: UV spectra and self-reaction kinetics of FCO and $FC(O)O_2$ and kinetics of some reactions of FCO_x with O_2, O_3, and NO at 296 K, J. Phys. Chem. 98 (1994) 2346–2356.
[10] T.J. Wallington, W.F. Schneider, D.R. Worsnop, O.J. Nielsen, J. Sehested, W. DeBruyn, J.A. Shorter, The environmental impact of CFC replacements HFCs and HCFCs, Environ. Sci. Technol. 28 (1994) 320A–326A.
[11] J. Sehested, T.J. Wallington, Atmospheric chemistry of Hydrofluorocarbon 134a. fate of the alkoxy radical trifluoromethoxy, Environ. Sci. Technol. 27 (1993) 146–152.
[12] F. Caralp, R. Lesclaux, A.M. Dognon, Kinetics of the reaction of CF_3 with O_2 over the temperature range 233–373 K, Chem. Phys. Lett. 129 (1986). 433-373.
[13] L. Yao, L. Du, M. Ge, D. Wang, Experimental and theoretical studies of the electronic structure and the ionization and dissociation Processes of trifluoromethyl peroxynitrate, J. Chem. Phys. 126 (2007). 184301-184301-7.
[14] M.P. Badenes, E. Castellano, C.J. Cobos, A.E. Croce, M.E. Tucceri, Rate coefficient for the reaction $FCO + FC(O)O_2 \rightarrow 2\ FC(O)O$ at 296 K, Chem. Phys. Lett. 303 (1999) 482–488.
[15] T. Nielsen, U. Samuelsson, P. Grennfelt, E.L. Thomsen, Peroxyacetyl nitrate in long-range transported polluted air, Nature 293 (1981) 553–555.
[16] H.B. Singh, Reactive nitrogen in the troposphere, Environ. Sci. Technol. 21 (1987) 320–327.

[17] R. Kopitzky, H. Willner, H.G. Mack, A. Pfeiffer, H. Oberhammer, IR and UV absorption cross sections, vibrational analysis, and the molecular structure of trifluoromethyl peroxynitrate, CF_3OONO_2, Inorg. Chem. 37 (1998) 6208–6213.
[18] R. Kopitzky, M. Beuleke, G. Balzer, H. Willner, Properties of trifluoroacetyl peroxynitrate, $CF_3C(O)OONO_2$, Inorg. Chem. 36 (1997) 1994–1997.
[19] A.G. Bossolasco, F.E. Malanca, G.A. Argüello, Photooxidation of $CF_3CF_2C(O)Cl$ in the presence of NO_2. Synthesis and characterization of pentafluoroethyl peroxynitrate, $CF_3CF_2OONO_2$, J. Photochem. Photobiol. A: Chem. 231 (2012) 45–50.
[20] M.P. Sulbaek Andersen, M.D. Hurley, T.J. Wallington, J.C. Ball, J.W. Martin, D.A. Ellis, S.A. Mabury, O.J. Nielsen, Atmospheric chemistry of C_2F_5CHO: reaction with Cl atoms and OH radicals, IR spectrum of $C_2F_5C(O)O_2NO_2$, Chem. Phys. Lett. 279 (2003) 28–36.
[21] G. Acerboni, N.R. Jensen, B. Rindone, J. Hjorth, Kinetics and products formation of the gas-phase reactions of tetrafluoroethylene with OH and NO radicals and ozone, Chem. Phys. Lett. 309 (1999) 364–368.
[22] M.J. Frisch, G.W. Trucks, H.B. Schlegel, G.E. Scuseria, M.A. Robb, J.R. Cheeseman, G. Scalmani, V. Barone, B. Mennucci, G.A. Petersson, H. Nakatsuji, M. Caricato, X. Li, H.P. Hratchian, A.F. Izmaylov, J. Bloino, G. Zheng, J.L. Sonnenberg, M. Hada, M. Ehara, K. Toyota, R. Fukuda, J. Hasegawa, M. Ishida, T. Nakajima, Y. Honda, O. Kitao, H. Nakai, T. Vreven, J.A. Montgomery, Jr., J.E. Peralta, F. Ogliaro, M. Bearpark, J.J. Heyd, E. Brothers, K.N. Kudin, V.N. Staroverov, R. Kobayashi, J. Normand, K. Raghavachari, A. Rendell, J.C. Burant, S.S. Iyengar, J. Tomasi, M. Cossi, N. Rega, J.M. Millam, M. Klene, J.E. Knox, J.B. Cross, V. Bakken, C. Adamo, J. Jaramillo, R. Gomperts, R.E. Stratmann, O. Yazyev, A.J. Austin, R. Cammi, C. Pomelli, J.W. Ochterski, R.L. Martin, K. Morokuma, V.G. Zakrzewski, G.A. Voth, P. Salvador, J.J. Dannenberg, S. Dapprich, A.D. Daniels, O. Farkas, J.B. Foresman, J.V. Ortiz, J. Cioslowski, D.J. Fox, Gaussian 09, Revision A.02, Gaussian Inc, Wallingford, CT, 2009.
[23] M.J. Frisch, J.A. Pople, J.S. Binkley, Self-consistent molecular orbital methods 25. Supplementary functions for Gaussian basis sets, J. Chem. Phys. 80 (1984) 3265–3269. and references therein.
[24] A.D. Becke, Density-functional thermochemistry. III. The role of exact exchange, J. Chem. Phys. 98 (1993) 5648–5652.
[25] A.D. Becke, Density-functional exchange-energy approximation with correct asymptotic behavior, Phys. Rev. A 38 (1988) 3098–3100.
[26] C. Lee, W. Yang, R.G. Parr, Development of the Colle–Salvetti correlation-energy formula into a functional of the electron density, Phys. Rev. B 37 (1988) 785–789.
[27] Y. Zhao, D.G. Truhlar, The M06 suite of density functionals for main group thermochemistry, thermochemical kinetics, noncovalent interactions, excited states, and transition elements: two new functionals and systematic testing of four M06-class functionals and 12 other functionals, Theor. Chem. Account 120 (2008) 215–241.
[28] A.G. Baboul, L.A. Curtiss, P.C. Redfern, K. Raghavachari, Gaussian-3 theory using density functional geometries and zero-point energies, J. Chem. Phys. 110 (1999) 7650–7657.
[29] L.A. Curtiss, P.C. Redfern, V. Rassolov, G. Kedziora, J.E. Pople, Extension of Gaussian-3 theory to molecules containing third-row atoms K, Ca, Ga–Kr, J. Chem. Phys. 114 (2001) 9287–9295.
[30] L.A. Curtiss, P.C. Redfern, K. Raghavachari, Gaussian-4 theory using reduced order perturbation theory, J. Chem. Phys. 127 (2007). 124105–124105-8.
[31] M.P. Badenes, L.L.B. Bracco, C.J. Cobos, Theoretical study of the equilibrium structure, vibrational spectrum, and thermochemistry of the peroxynitrate $CF_2BrCFBrOONO_2$, J. Phys. Chem. A 115 (2011) 7744–7752.
[32] M.P. Badenes, C.J. Cobos, Quantum chemical study of the atmospheric $C_2H_5C(O)OONO_2$ (PPN) molecule and of the $C_2H_5C(O)OO$ and $C_2H_5C(O)O$ radicals, J. Mol. Struct. Theochem. 856 (2008) 59–70.
[33] M.P. Badenes, M.E. Tucceri, C.J. Cobos, Theoretical study of the molecular conformations, vibrational frequencies and thermochemistry of the $FC(O)OOO(O)CF$, $FS(O_2)OOO(O_2)SF$ and $FC(O)OOO(O_2)SF$ trioxides, Comput. Theor. Chem. 1009 (2013) 86–93.
[34] A.P. Scott, L. Radom, Harmonic vibrational frequencies: an evaluation of Hartree−Fock, Møller−Plesset, quadratic configuration interaction, density functional theory, and semiempirical scale factors, J. Phys. Chem. 100 (1996) 16502–16513.
[35] A.G. Bossolasco, F.E. Malanca, M.A. Paci, G.A. Argüello, Mechanism of photo-oxidation of heptafluorobutyric anhydride in the presence of NO_2. Synthesis and characterization of heptafluoropropyl peroxynitrate, $CF_3CF_2CF_2OONO_2$, J. Phys. Chem. A 116 (2012) 9904–9910.
[36] W.J. Hehre, L. Radom, P.v:R. Schleyer, J.A. Pople, Ab Initio Molecular Orbital Theory, Wiley, New York, 1986.
[37] R.J. Berry, D.R.F. Burgess Jr., M.R. Nyden, M.R. Zachariah, M. Schwartz, Halon thermochemistry: ab initio calculations of the enthalpies of formation of fluoromethanes, J. Phys. Chem. 99 (1995) 17145–17150.
[38] J.W. Ochterski, Thermochemistry in Gaussian. <http://www.gaussian.com/g_whitepap/thermo.htm>.
[39] L.A. Curtiss, P.C. Redfern, D.J. Frurip, Theoretical methods for computing enthalpies of formation of gaseous compounds, in: K.B. Lipkowitz, D.B. Boyd (Eds.), Reviews in Computational Chemistry, vol. 15, Wiley-VCH, New York, 2000, pp. 147–211.
[40] M.P. Badenes, C.J. Cobos, Ab initio and DFT study of the molecular conformations and the thermochemistry of the CH_2=$CHC(O)OONO_2$ (APAN) atmospheric molecule and of the CH_2=$CHC(O)OO$ and CH_2=$CHC(O)O$ radicals, J. Mol. Struct. Theochem. 814 (2007) 51–60.
[41] F. Caralp, R. Lesclaux, M.T. Rayez, J.C. Rayez, W. Forst, Kinetics of the combination reactions of chlorofluoromethylperoxy radicals with NO_2 in the temperature range 233–373 K, J. Chem. Soc., Faraday Trans. 2 (84) (1988) 569–585.
[42] S.P. Sander, R.R. Friedl, J.R. Barker, D.M. Golden, M.J. Kurylo, P.H. Wine, J.P.D. Abbatt, J.B. Burkholder, C.E. Kolb, G.K. Moortgat, R.E. Huie, V.L. Orkin, Chemical Kinetics and Photochemical Data for Use in Atmospheric Studies, NASA/JPL Data Evaluation, JPL Publication 06-2, Evaluation No. 17, NASA, Pasadena, CA, 2011. <http://jpldataeval.jpl.nasa.gov>.